Experimental Demonstration of 128-SP-QAM in Uncompensated Long-Haul Transmission

2012 Optical Fiber Communication Conference and Exposition and the National Fiber Optic Engineers Conference, OFC/NFOEC 2013, Anaheim, 17-21 March 2013

Citation for the published paper:
Eriksson, T. ; Sjödin, M. ; Andrekson, P. (2013) "Experimental Demonstration of 128-SP-QAM in Uncompensated Long-Haul Transmission". 2012 Optical Fiber Communication Conference and Exposition and the National Fiber Optic Engineers Conference, OFC/NFOEC 2013, Anaheim, 17-21 March 2013

Experimental Demonstration of 128-SP-QAM in Uncompensated Long-Haul Transmission

Tobias A. Eriksson, Martin Sjödin, Peter A. Andrekson, and Magnus Karlsson
Photonics Laboratory, Department of Microtechnology and Nanoscience, Chalmers University of Technology, SE-412 96 Göteborg, Sweden
tobias.eriksson@chalmers.se

Abstract: We demonstrate 128-SP-QAM experimentally for the first time and compare the performance to PM-16QAM at the same symbol rate (10.5 Gbaud). We find a 1.7 dB increased sensitivity and 50% increased transmission reach over PM-16QAM.

OCIS codes: (060.4080) Modulation; (060.0060) Fiber optics and optical communications.

1. Introduction

Ever since the interest in coherent optical transmission systems was renewed, modulation formats that take advantage of both quadratures of the optical field as well as both polarization states have received a lot of attention due to the possibility to achieve high spectral efficiency (SE). Polarization multiplexed quadrature phase-shift keying (PM-QPSK) and polarization multiplexed 16-ary quadrature amplitude modulation (PM-16QAM) are examples of modulation formats commonly used to achieve an increased SE over long-haul transmission systems.

With traditional polarization multiplexed formats such as PM-16QAM and PM-QPSK, the constellations in the two polarization states are treated independently. However, formats that are optimized in the four-dimensional (4D) signal space spanned by the two quadratures and the two polarization states have recently been subject to a significant amount of research, mostly due to the higher sensitivity that can be achieved [1]. Examples of such 4D-modulation formats that has been implemented experimentally are polarization-switched QPSK (PS-QPSK) [2, 3] and 6-ary polarization-shift keying QPSK (6Pol-QPSK) [4, 5].

In the same manner as PS-QPSK can be derived from PM-QPSK, 4D-modulation formats can be derived from rectangular PM-16QAM. By using set-partitioning (SP) [6] on rectangular PM-16QAM constellations, modulation formats with higher sensitivities can be realized with a minor addition to the complexity of a standard PM-16QAM transmitter. One such format is set-partitioning 128-ary polarization-multiplexed 16QAM (128-SP-QAM), where the symbols are chosen from a standard Gray-coded PM-16QAM symbol alphabet with maintained parity, thus giving a $\sqrt{2}$ increase in the minimum Euclidean distance between the symbols compared to PM-16QAM [7, 8]. However, this comes at the cost of transmitting 7 bits per symbol instead of 8. 128-SP-QAM has in numerical investigations been shown to achieve more than 40% increased transmission reach compared to PM-16QAM [9, 10].

In this paper, we present the first experimental demonstration of 128-SP-QAM and compare the performance to Gray-coded PM-16QAM at the same symbol rate of 10.5 Gbaud. We transmit both formats over long-haul distances of uncompensated standard single mode fiber (SSMF) and quantify the increase in transmission reach provided by 128-SP-QAM.

2. Experimental Setup

The experimental setup is shown in Fig. 1. The transmitter is based on two IQ-modulators, one for each polarization. The eight 10.5 Gbit/s binary driving signals, pseudo random binary sequences (PRBS) with the length of $2^{15}-1$, are generated using three different pulse pattern generators (PPG1-3). The binary signals are combined in pairs with different amplitudes using two-way power combiners to generate the 4-level driving signals. The set-partitioning is achieved by programming the binary sequence from PPG3 as an XOR operation on the other seven binary bit sequences, resulting in a constant parity. The patterns from the three PPGs could not be synchronized electronically and when a pattern was loaded in PPG3, the reference to PPG1 and PPG2 was lost and therefore a variable delay, ΔT, of several thousands of bits had to be used for PPG3. This is implemented by modulating the binary sequence onto an optical wave using a Mach-Zehnder modulator (MZM) followed by a fiber of suitable length. The correct delay was found by monitoring the detected bit sequences in the receiver. The delayed pattern is amplified and then detected

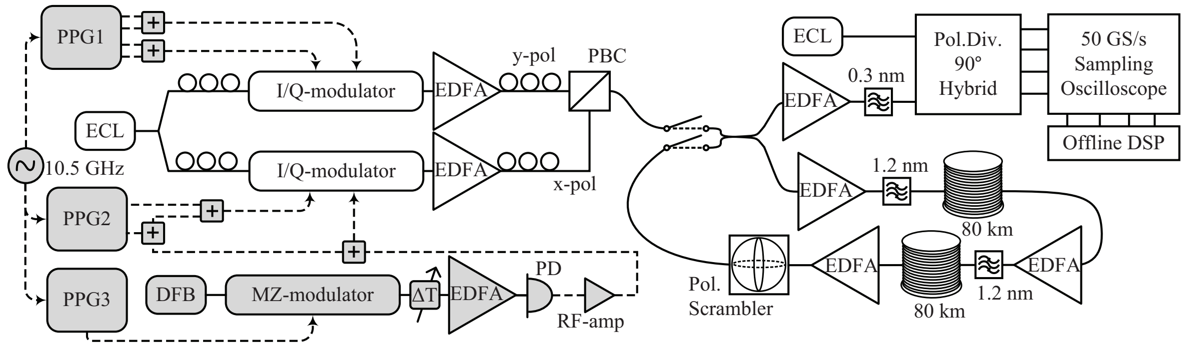

Fig. 1. Experimental setup for generation of 10.5 Gbaud PM-16QAM and 128-SP-QAM, recirculating loop and coherent receiver. Components used to generate electrical driving signals are marked with gray.

using a photo receiver. The electrical signal is amplified before being combined with another binary signal from PPG2 to drive the x-polarization I/Q-modulator. For PM-16QAM the same setup is used but with standard PRBS data from PPG3. It should be noted that this solution reduces the quality of the signal slightly and hence the performance is somewhat different for the two polarizations which can also be observed in the constellation plots in Fig. 2. A 1550 nm external cavity laser (ECL) with a linewidth of ∼100 kHz is used as a light source and the optical signal after each IQ-modulator is amplified by an Erbium-doped fiber amplifier (EDFA) before being combined with orthogonal polarization states using a polarization beam combiner (PBC).

The signal was then launched into a recirculating loop with two spans of 80 km SSMF with 17 dB loss each. Each span is followed by an EDFA with ∼5 dB noise figure to compensate for the loss and preceded by a 1.2 nm optical bandpass filter to suppress the amplified spontaneous emission (ASE) noise. A loop-synchronous polarization scrambler is implemented to avoid accumulated polarization impairments. Moreover, a third EDFA compensates for the loss of the polarization scrambler and the loop switching components. The noise from this EDFA is negligible.

In the receiver the signal is amplified by an EDFA followed by a 0.3 nm optical bandpass filter. The signal is then detected using a polarization diversity 90° optical hybrid with integrated balanced photo receivers and a ∼300 kHz ECL as local oscillator (LO). The output electrical signals are digitized using a 50 GS/s sampling oscilloscope with 16 GHz bandwidth and are later processed offline using a computer.

The digital signal processing (DSP) starts with a 7.35 GHz Bessel filter followed by optical front-end compensation. The signals are then re-sampled to two samples per symbol and a static finite impulse response (FIR) filter compensates for the accumulated dispersion. Polarization demultiplexing and adaptive equalization is performed with four 21-tap $T/2$-spaced FIR filters which are optimized using first the constant modulus algorithm (CMA) for pre-convergence, followed by the decision-directed least mean square (DD-LMS) algorithm for final adaptation. The frequency offset estimation, based on the fast Fourier transform (FFT), as well as the carrier phase estimation based on the blind phase search method with 64 test-phases [11], are performed within the DD-LMS loop. For 128-SP-QAM, a parity check is performed before the bit error rate (BER) is computed. The parity of each 8-bit symbol is computed and if it deviates from the sent parity, the most uncertain bit is inverted. Furthermore, the parity bit is also deducted before the BER is calculated. It should be noted that in this work the problem with phase and polarization ambiguity was not addressed. However, pilot symbol sequences, similar to what was used in [4], could be a possible solution to this problem.

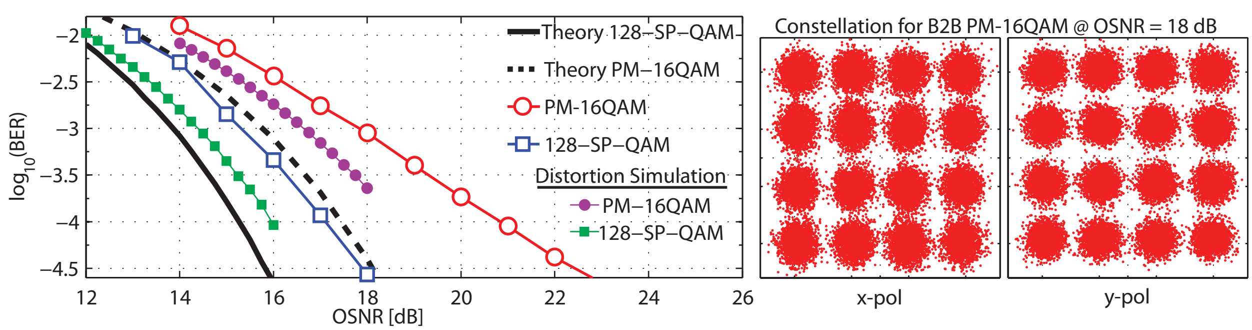

Fig. 2. Measured back to back performance of BER vs. OSNR for 10.5 Gbaud 128-SP-QAM (blue squares) and 10.5 Gbaud PM-16QAM (red circles) and theoretical performance for the same formats (solid and dashed line). Simulations with distortion in the rectangularity for 128-SP-QAM (small filled green squares) and PM-16QAM (small filled purple circles). Constellation diagrams for both polarizations of PM-16QAM at 18 dB OSNR are also shown.

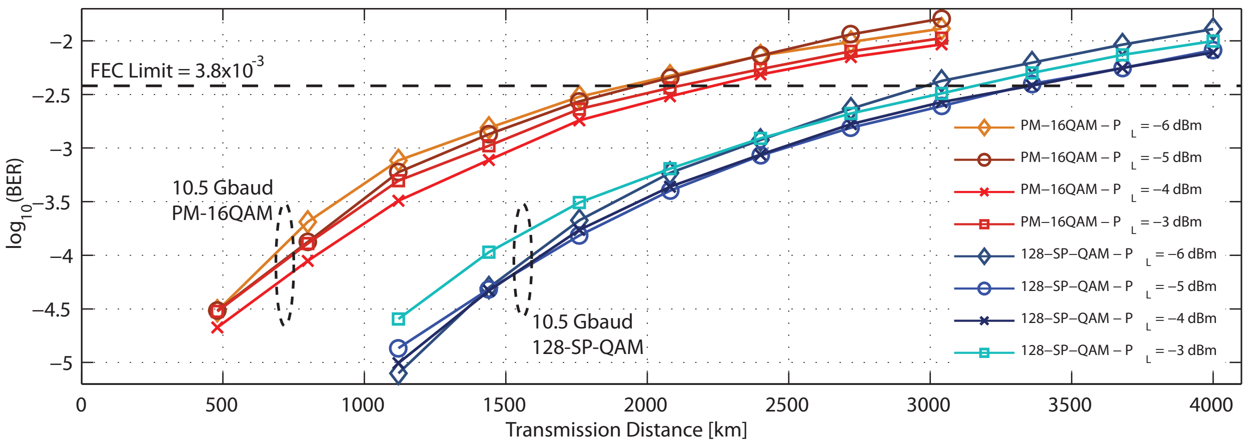

Fig. 3. Transmission results for 10.5 Gbaud PM-16QAM and 10.5 Gbaud 128-SP-QAM for different optical launch powers into the fiber spans. For PM-16QAM the optimal launch power for longest reach at the FEC limit is −4 dBm whereas for 128-SP-QAM both −4 dBm and −5 dBm yields similar reach.

3. Experimental Results

The back to back (B2B) performance for 10.5 Gbaud 128-SP-QAM (73.5 Gbit/s) and 10.5 Gbaud PM-16QAM (84.0 Gbit/s) are shown in Fig. 2. The implementation penalty at the forward error correction (FEC) limit of 3.8×10^{-3} was 1.5 dB for both formats and the relative sensitivity difference was 1.7 dB. The theoretical performance for 128-SP-QAM was found by Monte Carlo simulations with additive white Gaussian noise (AWGN) as the only impairment.

In Fig. 2, we also observe that PM-16QAM suffers a much higher penalty at lower BER compared to 128-SP-QAM. However, both theory and numerical simulations consider symbols on a perfectly rectangular grid which can be hard to achieve in experiments due to for instance; I/Q-modulator nonlinearities, bias drifts and non-ideal 4-level driving signals. We performed numerical B2B simulations where the constellations were distorted so that the center for different symbols had a minor offset from the rectangular grid, imitating what was seen in our experiments. The simulation results with distorted constellations are also included in Fig. 2 and we can confirm that deviations from the rectangular constellation affects PM-16QAM more than 128-SP-QAM, especially at lower BER. Hence, the degraded performance of PM-16QAM at lower BER in our experiments is attributed to the deviation from a perfectly rectangular grid caused by the transmitter. We also observe a tendency for a BER-floor for PM-16QAM at BER lower than 10^{-5}.

The transmission results for different launch powers are shown in Fig. 3. We defined the transmission reach as the crossing point at the FEC limit. For PM-16QAM the optimal launch power for maximum reach was −4 dBm whereas for 128-SP-QAM both −4 dBm and −5 dBm give approximately the same reach. The maximum reach was found to be 2200 km for PM-16QAM and 3300 km for 128-SP-QAM, i.e. at the same symbol rate we were able to achieve a 50% increase in the maximum transmission reach for 128-SP-QAM compared to PM-16QAM. This is in good agreement with the numerical simulation results in [9]. It should be noted that switching from PM-16QAM to 128-SP-QAM reduces the number of bits per symbol by one. However, in [9] it has been shown that 128-SP-QAM should have a significant increase in reach even at the same bit rate as PM-16QAM, which we intend to verify experimentally in future work.

4. Conclusions

We have presented the first experimental demonstration of 128-SP-QAM and compared the results to Gray-coded PM-16QAM at the same symbol rate of 10.5 Gbaud. We shown a sensitivity gain of 1.7 dB for 128-SP-QAM compared to PM-16QAM. We transmitted both formats over an uncompensated SSMF link and showed a 50% increase in the maximum reach for 128-SP-QAM (3300 km) compared to PM-16QAM (2200 km).

References

1. E. Agrell and M. Karlsson, *J. Lightwave Technol.*, vol. 27, no. 22, pp. 5115-5125, 2009.
2. M. Sjödin et al., *Opt. Exp.*, vol. 19, No. 8, pp. 7839-7846, 2011.
3. M. Nölle et al., *Opt. Exp.*, vol. 19, No. 24, pp. 24370-24375, 2011.
4. J. K. Fischer et al., *ECOC'12*, Paper We.1.C.4, 2012.
5. F. Buchali and H. Bülow, *ECOC'12*, Paper We.3.A.1, 2012.
6. G. Ungerboeck, *IEEE Trans. on Inf. Theory*, vol IT-28, no 1, 1982.
7. L. D. Coelho and N. Hanik, *ECOC'11*, Paper Mo.2.B.4, 2011.
8. M. Karlsson and E. Agrell, *OFC'12*, Paper OTu2C, 2012.
9. M. Sjödin et al., *Opt. Exp.*, vol. 20, No. 8, pp. 8357-8366, 2011.
10. J. Renaudier et al.,*ECOC'12*, Paper We.1.C.5, 2012.
11. T. Pfau et al, *J. Lightwave Technol.*, vol. 27, no. 8, pp. 989-999, 2009.